

Vaginal Mucosal Melanoma Cell Activation in Response to Photon or Carbon Ion Irradiation

Alexandra Charalampopoulou (MSc)^{1,2,*}, Amelia Barcellini (MD)^{3,4}, Margarita Bistika (MSc)⁵, Giovanni Battista Ivaldi (MD)⁶, Sara Lillo (MD)³, Giuseppe Magro (PhD)⁷, Ester Orlandi (MD)^{3,8}, Marco Giuseppe Pullia (PhD)⁹, Sara Ronchi (MD)³, Paola Tabarelli De Fatis (MSc)¹⁰, Angelica Facchetti (PhD)¹

¹ Radiobiology Unit, CNAO National Center for Oncological Hadrontherapy, Pavia, Italy

² University School for Advanced Studies IUSS, Pavia, Italy

³ Radiation Oncology Unit, Clinical Department, CNAO National Center for Oncological Hadrontherapy, Pavia, Italy

⁴ Department of Internal Medicine and Therapeutics, University of Pavia, Pavia, Italy

⁵ Department of Biology and Biotechnology "L. Spallanzani", University of Pavia, Pavia, Italy

⁶ Radiation Oncology Unit, Istituti Clinici Scientifici Maugeri IRCCS, Pavia, Italy

⁷ Medical Physics Unit, Clinical Department, CNAO National Center for Oncological Hadrontherapy, Pavia, Italy

⁸ Department of Clinical, Surgical, Diagnostic and Pediatric Sciences, University of Pavia, Pavia, Italy

⁹ Research and Development Department, CNAO National Center for Oncological Hadrontherapy, Pavia, Italy

¹⁰ Medical Physics, Istituti Clinici Scientifici Maugeri IRCCS, Pavia, Italy

ARTICLE INFO

Keywords:

Mucosal malignant melanoma
Radiobiology
Melanin
Migration
Carbon ions

ABSTRACT

Purpose: Primary gynecological melanomas are uncommon with lower survival rates compared to cutaneous melanomas. Although melanocytes have been identified in a variety of mucosal membranes, little is known about their interactions or roles inside the mucosa layer. Melanin is a common pigment in nature and is endowed with several peculiar chemical, paramagnetic, and semiconductive characteristics. One of its latest explored functions is its interaction with ionizing radiation as a protective mechanism as well as its implication in the metastatic cascade of tumor cells.

Materials and Methods: In this work, we analyzed in vitro the effects of different doses of photon and carbon ion irradiation on dendrite formation, pigmentation, migration, and invasion abilities of human mucosal melanoma cells of the vagina. We evaluated the morphology and melanin production of HMV-II cells exposed to photon and carbon ion beams with single doses between 0.5 and 10 Gy.

Results: Our results showed that irradiation induces dendrite formation or elongation and pigmentation in HMV-II cells in a dose-type-dependent and radiation-type-dependent way but also a decrease in cell motility.

Conclusion: The present study describes for the first time an induction of dendritic formation, melanin production, and alterations in migration and invasion abilities by low-linear energy transfer and high-linear energy transfer radiation in human mucosal melanoma cells, suggesting a radioprotective response to further possible exposures increasing the radioresistance of these cells.

Introduction

Melanocytes found in the mucosal membranes of the respiratory, gastrointestinal, and urogenital tracts are the source of primary mucosal melanomas. Gynecological melanomas are uncommon, with the vulva as the most frequent site, and are known to exhibit more aggressive behavior and have a worse prognosis than other melanoma

subtypes. Due to the localization of the majority of these mucosal melanomas and the absence of early, distinct signs, a poor prognosis and delayed detection are common.¹ Among gynecological melanomas, vaginal ones have a dismal overall survival (OS) that ranges between 0% and 32% at 5 years.^{2,3} Currently, there is no consensus or guidelines about the management of this rare disease, but surgery, when feasible. However, considering the short time to progression after demolitive

* Corresponding author. Radiobiology Unit, CNAO National Center for Oncological Hadrontherapy, Erminio Borloni 1, 27100 Pavia, Italy.
E-mail address: alexandra.charalampopoulou@cnao.it (A. Charalampopoulou).

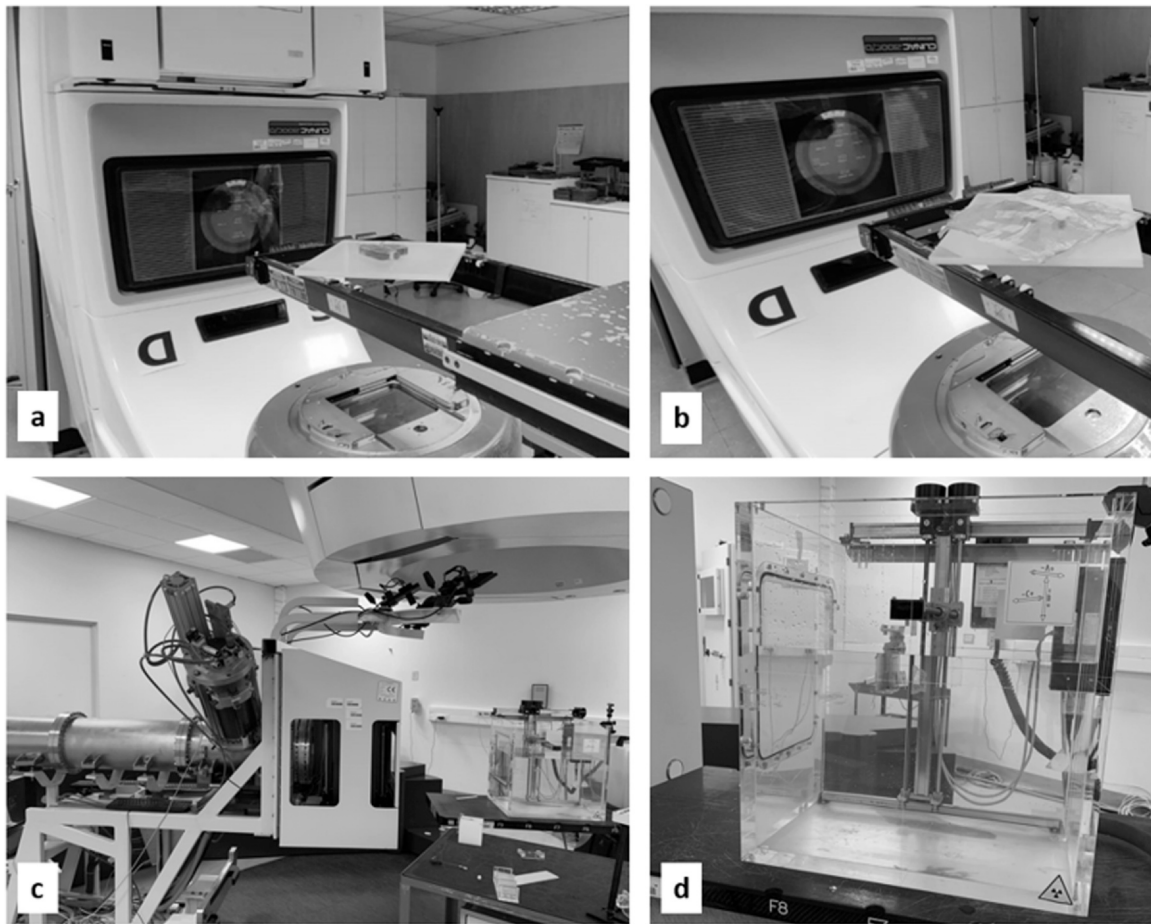


Figure 1. Experimental setups for (a and b) photon irradiation and (c and d) carbon ion irradiation.

surgery and the morbidity due to extensive surgical approaches, a more conservative approach aimed also to control the symptoms might be justified.³⁻⁵ Unfortunately, the intrinsic radioresistance of this histology makes conventional photon beam radiation therapy unsatisfactory. However, the preliminary experiences with carbon ion radiation therapy achieved really promising results both in terms of local control and in OS,⁶⁻⁸ with a high safety profile also in case of combination of immunotherapy.⁶ The rationale of the use of carbon ion irradiation (CIRT) in radioresistant malignancies is due to its ballistic properties that allow increasing the total dose to the target, but above all, to the radiobiological hallmarks. Indeed, CIRT is less cell cycle-dependent, has a high relative biological effectiveness, and acts independently on the hypoxic status of the tumor.⁹ Moreover, the DNA damages caused by CIRT are able to regulate several molecular pathways, increasing also the immunogenic cell death.¹⁰ However, the damage to normal tissues and the emergence of different tumor radioresistance mechanisms frequently restrict the effectiveness of RT.¹¹⁻¹³ Cancer cells, such as melanomas, may survive by taking advantage of their activation mechanisms that involve morphological changes, compensatory survival signaling, damage-repair signaling (eg, reactive oxygen species [ROS] scavenging), DNA repair, unfolded protein response, and the induction of autophagy.¹⁴⁻¹⁶ Moreover, the presence of melanin pigments is considered one of the possible mechanisms of intrinsic radioresistance,¹⁷⁻¹⁹ considering its ability to face melanogenesis to scavenge free radicals and ROS.^{20,21} Furthermore, *in vitro* and *in vivo* experiences showed the inhibition of trans-migration mediated by melanin, suggesting an important role on the control of metastatic potential.²²⁻²⁷ Cancer cells take on an invasive, migrating phenotype that causes them to invade nearby tissues, enter the bloodstream, and travel to far-off locations.²⁸ Research generally shows that, while CIRT reduces this

in several cell lines, photon radiation (XRT) may subsequently activate a wide variety of intracellular signaling pathways, increasing the motility and/or invasiveness of tumor cells.²⁹ However, not all cell lines react to radiation in the same way. For example, some cell lines showed decreased invasiveness in response to photon radiation, while others showed increased invasion in response to carbon ion radiation.³⁰⁻³² Melanoma cells' capacity to undergo phenotypic or functional switches in response to environmental changes following radiation exposure makes them an excellent model for researching the activation of cancer.

Although a few studies analyzed the radio-response of skin melanoma cells, finding a correlation between melanin content and radioresistance,^{33,34} to the best of our knowledge, there have been no studies that investigated the effects of low-linear energy transfer (LET) or high-LET radiation to cell activation in terms of dendricity, melanin production, and migration or invasion of mucosal melanoma cells. Herein, we analyzed *in vitro* the effects of different doses of XRT and CIRT on dendrite formation and elongation, as well as on melanin pigment appearance and motility abilities of human mucosal melanoma cells of the vagina.

Materials and methods

Cells and reagents

The human melanoma vaginal cell line, designated HMV-II, was acquired from Sigma Aldrich, located in St. Louis, MO, USA. The cells were cultivated in RPMI 1640 media supplemented with 10% heat-inactivated fetal bovine serum, 100 U/mL penicillin, and 0.1 mg/mL streptomycin in a humidified chamber with 5% CO₂. Employing 10%

trypsin, cells were regularly divided once they had reached 80% to 85% of confluence up to passage 10. The culture medium and all additives were bought from Sigma Aldrich.

Irradiations

HMV-II cells that were cultivated exponentially in T12.5 or T25 culture flasks (Corning) were subjected to photon or C-ion beams at doses of 0.5, 1, 2, 4, 6, 8, or 10 Gy. Every fake sample that had been exposed to radiation was treated the same as the real samples and placed on a surface in an adjacent room. To guarantee electronic balance with the employed beams, which began from below (180°), T25 flasks were placed horizontally above a 1.5 cm-thick layer of Plexiglas and coated with a 1 cm-thick layer of water-equivalent bolus. Photon radiation was carried out with a 6 MV from a LINAC linear accelerator (3 Gy/min as dose rate) in the Radiation Oncology Unit of the Istituti Clinici Scientifici Maugeri of Pavia, Italy (Figure 1a and b).

A fixed horizontal beamline at the National Center for Oncological Hadrontherapy in Pavia, Italy, was used to deliver active-scanning carbon ion beams. T12.5 flasks were positioned within a water phantom with its entrance window at the room isocenter and filled with a non-complete cell culture medium, leaving an air gap at the very top of the flask only. This configuration created a full liquid-to-plastic continuous interface at the irradiation window. To achieve a uniform dose region with a thickness of 6 cm, a spread-out Bragg peak (SOBP) was generated by superimposing 31 different beam energies (ranging from 246 to 312 MeV/n, corresponding to a water-equivalent path length of 120 to 180 mm with 2-mm increments in depth). This SOBP was designed to be homogeneous in physical dose to minimize any potential dose gradients across the cell monolayer, consistent with standard practice in clonogenic assays; thus, no radiobiological model was employed at this stage. We recalculated the plan using our clinically commissioned treatment planning system (RaySearch RayStation v 2023B) to verify the flatness of the dose distribution along the SOBP. The homogeneity was further confirmed through ionization chamber dosimetry (calibrated Farmer chamber) placed at various depths within the irradiation field. The chosen SOBP extensions can be representative of clinically adopted irradiation beams. The LET distribution, ranging from about 32 to 140 keV/ μm in the modulated 6 cm region, was also extracted from the TPS, showing a value of 44.5 keV/ μm at the position of the flasks. Reference dosimetry is reported in Rossi et al.³⁵

The cells were positioned 15 cm below the phantom's surface, roughly in the middle of the SOBP (Figure 1c and d). The noncomplete medium was removed immediately after the radiation was concluded, and 5 mL of the complete medium was added for the incubation process. For every condition, at least 3 samples were used.

Melanocyte morphology and melanin synthesis

By applying a phase-contrast microscope (BX1, Olympus), images of representative fields of both control and irradiated flasks were captured every day for 10 days following the administration of radiation to record the length, dendritic development, and pigmentation of the melanocytes at 100X magnification. Dendritic cells were cells that had one or more thin processes that extended beyond the width of the cell body.³⁶ The starting point for measurement has been chosen at the point where the dendrite emerged from the soma. At least 5 distinct representative fields' worth of cells were assessed for each condition (dose and energy) of irradiation. The dendritic length was measured using the digital camera and expressed in millimicroliters. All raw data were normalized to the maximal value to eliminate units of measurement.

To evaluate melanin synthesis, separate samples were used compared to those used for dendrite length measurements. Melanin synthesis was surveyed by counting the number of pigmented (brownish) cells, by evaluating of pellets' color, and by absorbance measurements

of the pellet's supernatants collected 10 days after exposure to irradiation using an Absorbance Reader (BioTek 800TM TS). More specifically, cells were cultured for 10 days after the exposure to irradiation. Both irradiated and control (mock-treated) HMV-II cells were collected by trypsinization and centrifuged in order to form pellets. The supernatant was discarded, and the pellets were washed twice with phosphate-buffered saline to remove any remaining media or trypsin. Each pellet contained 1 000 000 cells, which was achieved by counting the cells using the LUNA-II automatic cell counter to ensure even concentrations across all groups.

Holotomographic microscopy acquisitions

Label-free images were acquired using a 3D Cell Explorer-fluo microscope (Nanolive SA—in collaboration with Media System Lab Srl). A 520 nm laser is installed in the microscope to enable tomographic phase microscope, enabling label-free refractive index image acquisition at high resolution. Images were reconstructed using STEVE Software (STEVE, Nanolive SA) and FIJI. Nanolive 3D Cell Explorer-fluo is supplied for live cell imaging (Okolab, Incubator chamber with temperature, humidity, and gas control).

For imaging, 3000 nonirradiated and irradiated HMV-II cells were plated in 35 mm No.1.5 ibidi polymer coverslip bottom dishes. After 48 h, the dishes were put inside the incubator chamber of the microscope, and overnight imaging began, with the microscope acquiring every 30 s.

Cell migration

Cell migration was evaluated through in vitro Boyden chamber migration assay, using transwell inserts. Following irradiation, HMV-II cells were trypsinized and counted using the LUNA-II automated cell counter. A total of 100 000 mock-treated and irradiated cells were seeded in the upper inserts of a 24-multiwell culture plate (Corning). The lower chambers were filled with a medium containing 20% serum that acts as a chemoattractant, promoting the migration of cells through the 0.8 μm pores of the membrane toward the bottom. To ensure accurate measurement of migration, 24 h after incubation, the membrane of each insert was carefully cleaned with a cotton-tipped applicator to remove any residual media or nonmigrated cells that had not moved to the lower chamber. Cells that successfully migrated and were attached to the underside of the membrane underwent May-Grünwald-Giemsa staining after being fixed in 70% cold ethanol. Inserts were examined under a 200X phase-contrast microscope, and for each insert that corresponded to a given condition, pictures from at least 5 distinct fields were captured. All raw data were normalized to the maximal value to eliminate units of measurement.³⁷ For every condition, at least 3 separate replicates were carried out.

Cell invasion

Cell invasion was evaluated through in vitro invasion assay, using the BioCoat Matrigel Invasion Chamber (Corning). The 8.0 μm PET Membrane porous filters were conditioned by adding fresh growth medium both in the lower and in the upper chamber for 2 h. After the exposure to irradiation, HMV-II cells were trypsinized, and 10 000 irradiated and nonirradiated cells were seeded in the top inserts, while 20% serum-enriched medium was introduced to the bottom chambers to act as a chemoattractant for the cells. Each insert's membrane was thoroughly cleaned with a cotton-tipped applicator 24 h after incubation to carefully remove the media and any remaining cells. Fixing the invading cells required 70% cold ethanol, and the May-Grünwald-Giemsa stain was used. When the inserts were dry, they were examined using a 200X phase-contrast microscope, and for each insert that corresponded to a given condition, pictures from at least 5 distinct fields were captured. All raw data were normalized to the maximal value to eliminate units of measurement.³⁷ For every condition, we ran at least 3

separate replicates.

Statistics

All data are provided as the means ± SDs and estimated with GraphPad Prism software, version 8 (GraphPad Software Inc). For each condition, at least 3 independent biological replicates were conducted. The results from these replicates were combined to calculate the overall mean and SD for each experimental condition. The 2 groups were then compared for significant differences using a 2-tailed independent *t* test. A difference that was deemed statistically significant was indicated by *P*-values < .05. At least 3 replicates of each experiment were conducted.

Results

In our cell culture conditions, HMV-II cells maintained an epithelial morphology, with most of the cells presenting a triangular or spindle-like shape with short processes. After exposure to XRT or CIRT, HMV-II cells showed increased morphological activation, characterized by dendrite formation and elongated dendritic morphology, that resulted in being dose-type and radiation-type dependent (Figure 2a-c).

More specifically, already 24 h after the exposure to photons, the average dendrite length increased progressively to the increasing doses until 6 Gy where we observed the highest average dendrite length, while it decreased at higher doses of 8 and 10 Gy (Figure 2d). This morphology persisted during the entire time of culturing, up to 10 days. On the other hand, after 24 h of carbon ion irradiation, we did not observe such significant differences in the average dendrite length, but at the timepoint of 48 h, HMV-II cells displayed dendrite elongation that gradually increased with the exposure to increasing doses of CIRT. Also, in this case, the maximum average dendrite length was observed at 6 Gy (Figure 2e), while the trend remained the same up to 10 days postirradiation. However, XRT caused a more significant elongation of dendrite processes when compared to CIRT at all time points (Figure 2f).

Before exposure to irradiation, in our cell culture conditions, HMV-II cells did not present any brownish pigments, and after centrifugation,

the pellets of cell aggregates were white to gray. We observed the cells under the microscope up to 20 days after XRT or CIRT with intervals of 24 h. No pigmented cells were visible in the culture of sham-irradiated samples, while in the irradiated ones, the appearance of melanin pigments gradually increased, according to the dose received, since the most pigmented cells were visible at one of the highest doses (Figure 3a-c).

The first pigmented cells appeared 3 days after the exposure to XRT and 5 days after CIRT and the highest number was reached 10 days after exposure at 8 Gy in both cases, although with very different values (average of 96 cells versus 24, respectively) (Figure 3d-f). After this interval time, the numbers of brown cells remained constant.

Concerning the color of the pellets, which appeared white to gray in the case of control cultures, we observed that they turned light brown at the intermediate doses (from 0.5 to 6 Gy) to dark brown at 8 Gy (Figure 4), proving melanin synthesis, after both types of irradiation.

Similarly, the measurements of melanin absorbance highlighted that 10 days after irradiation, melanin synthesis is higher in the photon-irradiated cells when compared to the carbon ion-irradiated ones (Figure 5).

Using the transwell migration assay, we observed that after exposure to either XRT or CIRT, HMV-II cells' ability to migrate diminished in a dose-dependent manner, and the amount of migrated cells in exposed samples compared with control ones decreased with increasing the dose. When compared to cells exposed to photons, C-ions significantly reduced cell migration (ie, 0.77 in C-ion-irradiated cells compared to 0.89 in photon-irradiated cells at 2 Gy) (Figure 6a).

Regarding cell invasion, a similar pattern was observed. The number of invading cells 24 h postirradiation decreased after the exposure to photons or C-ions, and also, in this case, the effect was more significant after CIRT (ie, 0.48 in CIRT cells compared to 0.59 in photon beam radiation therapy cells at 4 Gy) (Figure 6b).

Discussion

The pathogenesis of mucosal melanomas is largely unknown and the subject of a current debate also due to different hallmarks and functions

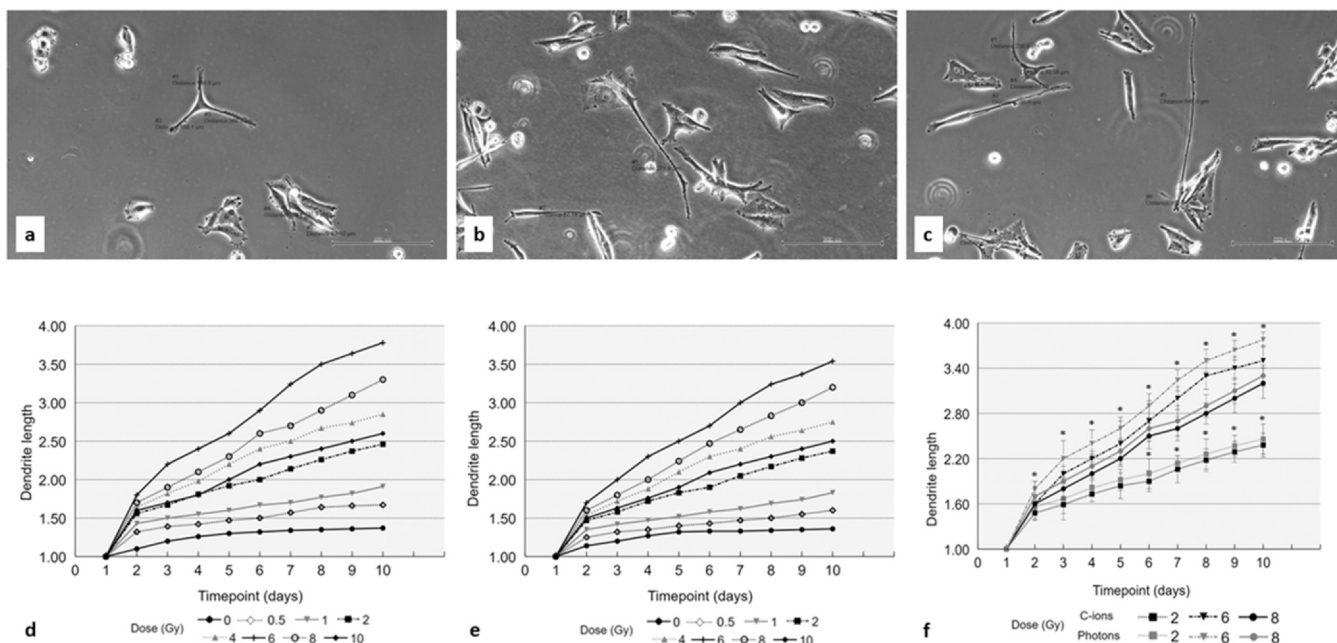


Figure 2. Dendritic processes of HMV-II cells at (a) normal conditions (no exposure to irradiation) and after the exposure to 6 Gy of (b) C-ions and (c) photons, obtained using a phase-contrast microscope at 100X magnification. (d) Normalized data of dendrite length after the exposure to photons and to (e) C-ions. (f) Comparison of dendrite length between photons and C-ions at 2, 6, and 8 Gy. *Stands for *P* ≤ .05 and a statistically significant difference between the 2 types of irradiation at 2, 6, and 8 Gy at each timepoint.

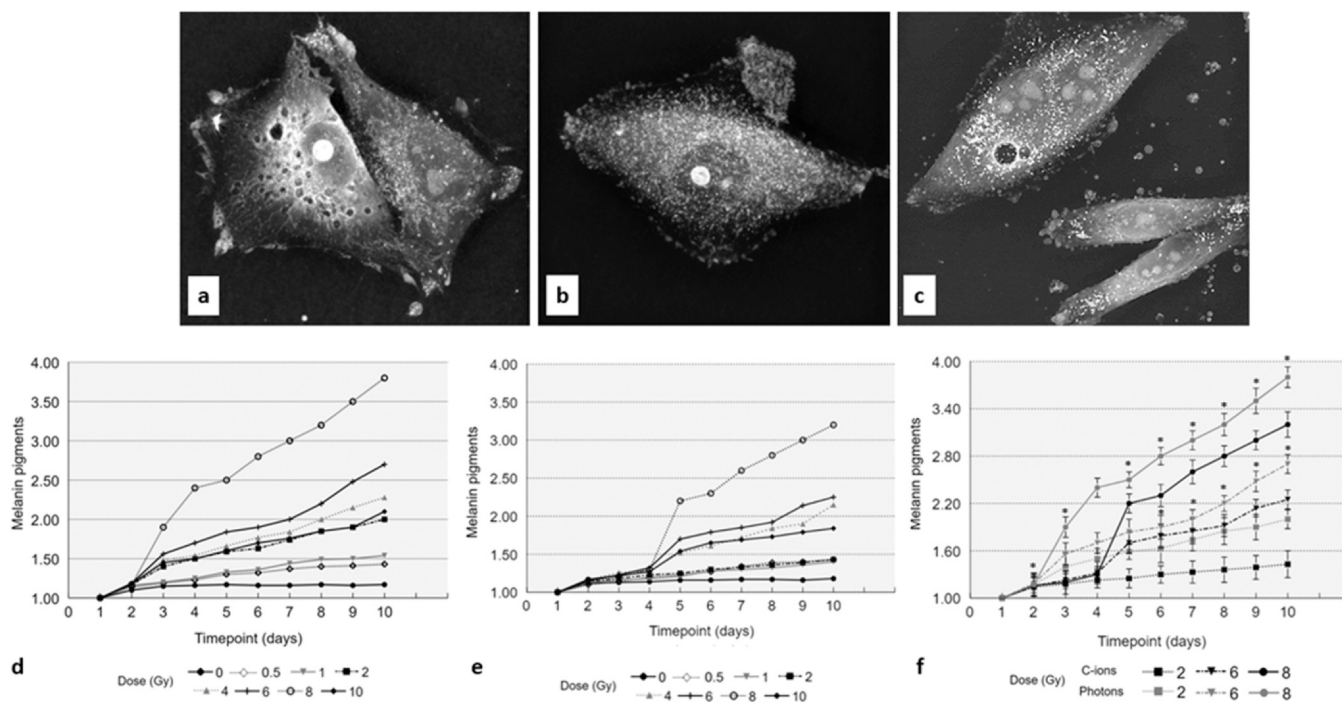


Figure 3. Label-free holotomographic images of HMV-II cells at (a) control condition and after the exposure to (b) 2 Gy and (c) 4 Gy of C-ions, obtained using the 3D Cell Explorer-fluo microscope. The white spots represent the melanosomes, which contain melanin. (d) Normalized data of melanin pigments after the exposure to photons and to (e) C-ions. (f) Comparison of melanin pigments between photons and C-ions at 2, 6, and 8 Gy. *Stands for $P \leq .05$ and a statistically significant difference between the 2 types of irradiation at 2, 6, and 8 Gy for each timepoint.

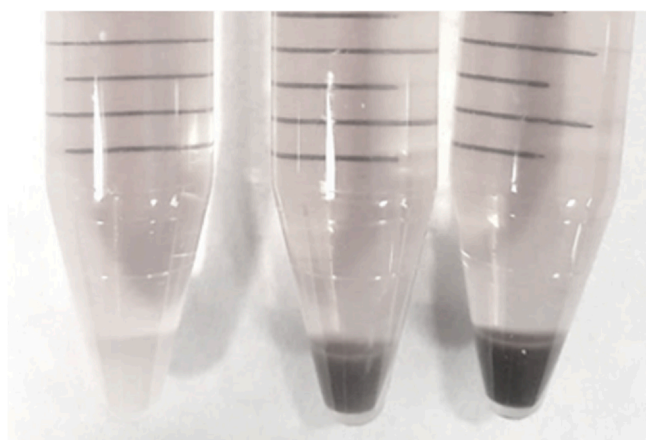


Figure 4. Pellets of HMV-II cells at control condition and after the exposure to 8 Gy of C-ions and photons (starting from the left).

of melanin in the skin and in the extracutaneous sites, although the similar embryological origin.³⁸ Besides the function of the skin melanin to protect the dermis from the damaging effects of sunlight by serving as a Ultraviolet (UV) radiation screen,³⁹⁻⁴⁴ melanin plays a role in the innate immunological defense system^{45,46} and also neutralizes ROS induced largely by Ultraviolet A radiation, by its antioxidant activity, and by free-radical scavenger effects.²¹ However, the capability of melanin pigment to shield healthy melanocytes from radiation and oxidative stress can also render melanoma cells unresponsive to many forms of treatment, such as irradiation.^{47,48} Dendricity in skin melanocytes is a decisive factor concerning epidermal pigmentation since dendritic extensions are essential for the relocation of melanosomes from melanocytes to the surrounding keratinocytes,⁴⁹ and it is promoted by UV irradiation.⁵⁰ On the other hand, the role of dendrites in mucosal melanocytes is not clear, and the cell type that dendrites are approaching, although the in-situ component of acral lentiginous and

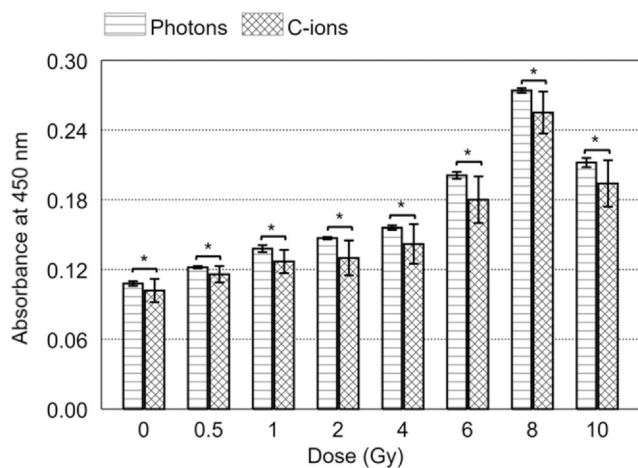


Figure 5. Melanin absorbance at 450 nm 10 days after the exposure to photons and C-ions. *Stands for $P \leq .05$ and a statistically significant difference.

mucosal malignant melanomas typically displays the dendritic architecture of malignant cells.^{51,52}

Considering this challenging background, the results of our study reveal intriguing insights into the morphological and functional changes exhibited by human mucosal melanoma cells of the vagina in response to XRT and CIRT. Under normal culture conditions, HMV-II cells displayed a characteristic epithelial morphology, but following exposure to both types of irradiation, a notable activation response was observed. The most prominent morphological change was the formation or elongation of dendritic processes. After XRT, there was a dose-dependent increase in dendrite length up to 6 Gy, with a subsequent decrease at higher doses. That could be probably explained by the cell damage induced after the exposure to 8 and 10 Gy of irradiation that caused the slight decrease in dendritic lengths observed. Similarly, CIRT induced dendrite elongation, peaking at 6 Gy. However, XRT

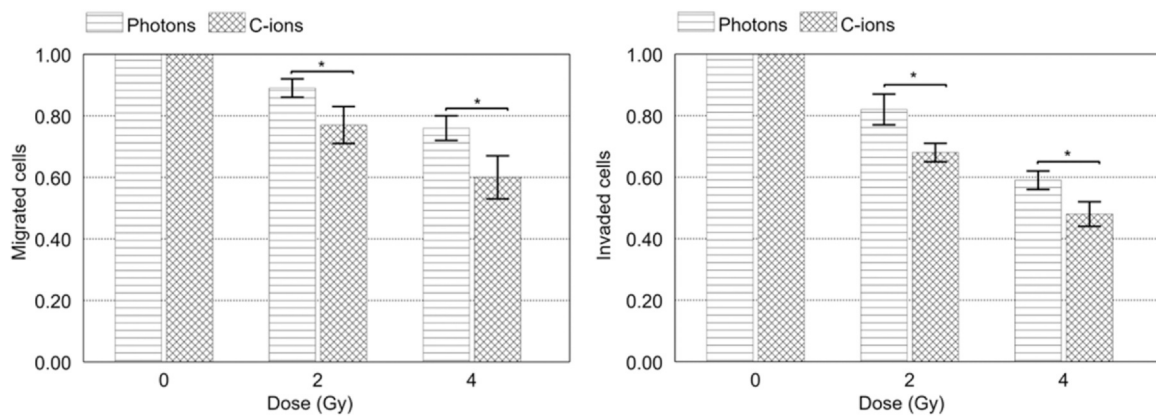


Figure 6. (a) Boyden chamber migration assay: migrated HMV-II cells after exposure to 2 and 4 Gy of photons or C-ions and (b) invasion assay: invaded HMV-II cells after exposure to 2 and 4 Gy of photons or C-ions. *Stands for $P \leq .05$ and a statistically significant difference.

resulted in more significant dendrite elongation than CIRT at both 24 and 48 h postirradiation.

Interestingly, the results of our experiments also highlight melanin synthesis activation in HMV-II cells by ionizing irradiation. Indeed, in our experimental conditions, mucosal melanoma cells exhibited an increased ability to synthesize melanin in a dose-dependent manner, with the appearance of pigmented cells and a color change in cell aggregates. The highest number of pigmented cells occurred 10 days after exposure to 8 Gy in both XRT and CIRT, suggesting a correlation between radiation dose and melanin synthesis. However, it is important to underline that photon irradiation seems to induce a more significant cell activation in terms of melanin synthesis when compared to exposure to carbon ions. These results are confirmed by measurements of the absorbance at 450 nm, which demonstrated a higher melanin production postirradiation that was higher after the exposure to photons when compared to carbon ions, presenting a peak at 8 Gy.

From a clinical point of view, literature data have shown that melanin formation is associated with a faster rate of disease progression and that the presence of melanin in metastatic melanoma cells reduces the effectiveness of radiation therapy.⁵³⁻⁵⁵ With regards to the biology aspect, it has been reported that melanin plays a role in decreasing radiosensitivity to low-LET (XRT) and high-LET (CIRT) irradiations of cutaneous melanoma cells,^{19,56} and melanized microbial organisms are particularly radioactively adapted to conditions including cooling pools of nuclear reactors, satellites, and the contaminated Chernobyl nuclear plant.⁵⁷ Besides, it is thought that one of the ways that fungus and tree frogs at Chernobyl zones acquire radioprotective qualities by means of enhanced melanin production^{58,59} (Figure 7).

The current hypothesis is that melanin carries out a scavenger activity against cytotoxic short-lived free radicals and consequently reduces DNA damage. But melanin synthesis seems to be related also to mechanisms of cell migration and invasion since there are studies which suggest that the presence of melanin could probably inhibit the metastases of melanoma.^{33,60} Thus, in addition to its UV protective function, melanin seems to play a role in preventing melanoma metastasis.

In parallel with our experiments regarding mucosal melanoma cell activation, we also investigated the impact of XRT and CIRT on cell migration and invasion capacities. Both types of irradiation led to a dose-dependent decrease in migration and invasion, with CIRT

demonstrating a more significant effect, as reflected in lower numbers of migrated and invading cells compared to XRT. Importantly, tumor cell migration and invasion play crucial roles in numerous processes, such as immune cell trafficking. This point is of utmost importance, considering that preclinical studies showed more efficient antitumor immune responses after CIRT compared to XRT.⁶¹⁻⁶³

Actually, it has been shown that melanin and the microphthalmia-associated transcription factor can reduce the aggressiveness of melanoma by inhibiting a number of critical metastatic processes,⁶¹ even though, to our knowledge, there are no studies that investigated the association of melanin synthesis and motility abilities of cells postirradiation. However, this is an interesting aspect that could be further investigated by performing experiments also with the cell line used in this study.

The present study has several undeniable limitations. First, the 2D experience lacks the complex interactions between cells and the extracellular matrix present in living tissues that might impact the cellular responses to radiation, including pigment production and motility, as well as dendritic formation and elongation. Moreover, the single cell line represents a limited biological context and the in vitro experiment, although a surrogate of the in vivo ones is limited by the intrinsic static condition different from a dynamic 3D and in vivo model. In addition, the absence of correlation between the molecular status of HMV-II cells and the response to low and high LET might be a possible bias. However, the methodology used, the different irradiation conditions tested, and the fact that, to the best of our knowledge, there are no data on the effect of low and high LET in terms of dendrite formation and elongation, as well as melanin pigment appearance and motility abilities of HMV-II, are the main strengths of our experiments.

The preliminary data obtained from the current experience pave the way to proceed with subsequent analyses involving more complex models (such as 3D or in vivo) that can confirm the 2D results in a nonstatic environment, capturing all the nuances of the processes evaluated in the current work, drawing near a real-world scenario. Moreover, including the molecular hallmarks, the cell-cell cross-talking, and the molecular background as possible predictive variables of response might help to move forward a better comprehension of this disease, with potential implications for therapeutic strategies and further exploration of the underlying mechanisms.

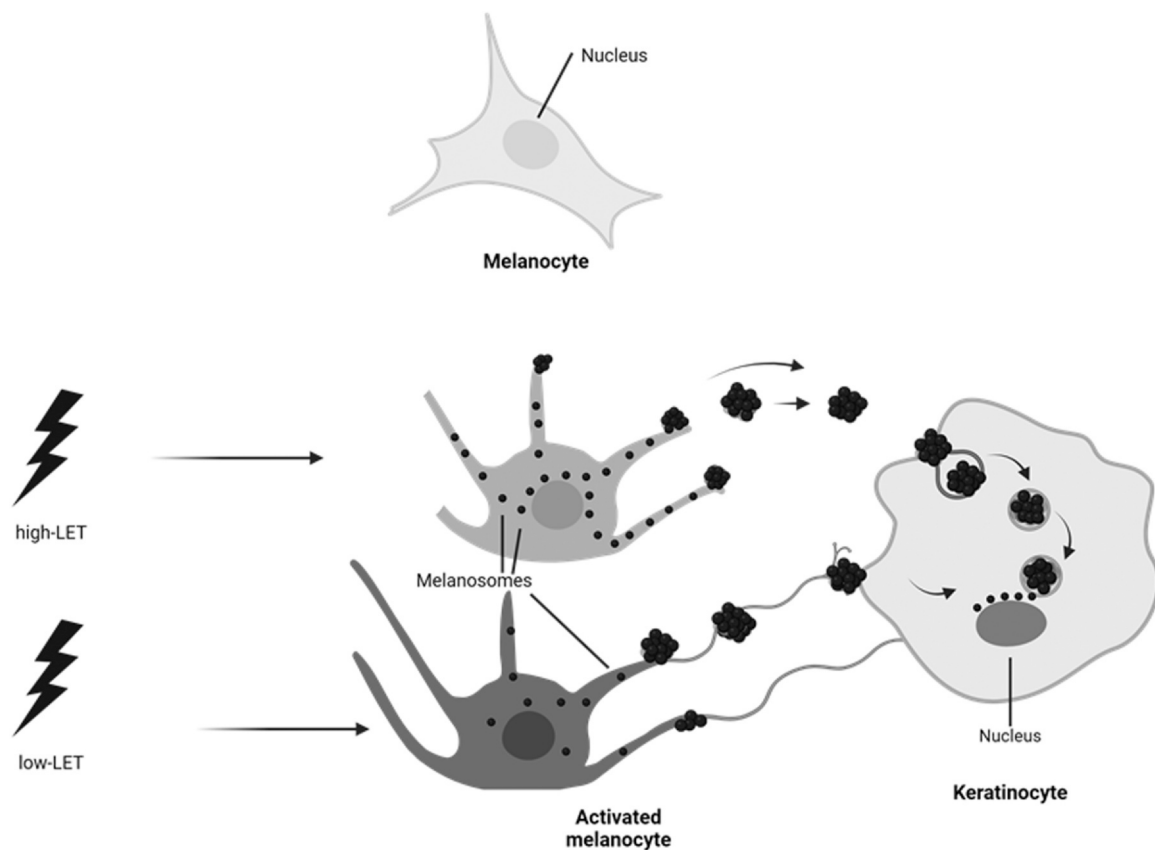


Figure 7. Possible mechanism of melanin synthesis for radioprotection.

Conclusions

The extent and nature of cell activation postirradiation depend on factors such as the dose of radiation, cell type, and the ability of the cells to repair damage. In conclusion, our study provides comprehensive insights into the cellular responses of HMV-II cells to XRT and CIRT in terms of morphological changes, characterized by dendrite formation and elongation, which suggest a distinctive activation response following irradiation, as well as in terms of melanin synthesis. This association between irradiation dose and melanin synthesis underscores the dynamic nature of cellular responses in mucosal melanoma cells.

Furthermore, our experiments into migration and invasion capacities revealed a dose-dependent decrease in both parameters after exposure to XRT and CIRT. Carbon ion irradiation exhibited a more substantial impact, emphasizing its potential efficacy in limiting the migratory and invasive capabilities of HMV-II cells.

Overall, despite the undeniable limitation of our findings limited to one cell line, our study paves the way for a better comprehension of the complex interplay between different irradiation types and cellular responses in mucosal melanoma. Understanding the mechanisms behind cell activation after irradiation is crucial for developing strategies to enhance the efficacy of radiation therapy or mitigate the adverse effects of radiation exposure.

Author Contributions

Alexandra Charalampopoulou and Angelica Facoetti conceptualized the study and wrote the first draft of the manuscript; Alexandra Charalampopoulou and Margarita Bistika performed the *in vitro* experiments; Giovanni Battista Ivaldi and Paola Tabarelli De Fatis assisted with photon irradiations and access to Maugeri Hospital; Giuseppe Magro and Marco Giuseppe Pullia supervised the dosimetry and the carbon ion irradiations; Angelica Facoetti and Amelia Barcellini performed data analysis;

Amelia Barcellini, Sara Ronchi, Sara Lillo, and Ester Orlandi critically revised the manuscript; Angelica Facoetti coordinated the study. All authors contributed to the article and approved the submitted version.

Declaration of Conflicts of Interest

The authors declare no conflict of interest.

Funding and Support

This research received no external funding.

References

- Mihajlovic M, Vlajkovic S, Jovanovic P, Stefanovic V. Primary mucosal melanomas: a comprehensive review. *Int J Clin Exp Pathol*. 2012;5(8):739–753.
- Gadducci A, Carinelli S, Guerrieri ME, Aletti GD. Melanoma of the lower genital tract: prognostic factors and treatment modalities. *Gynecol Oncol*. 2018;150(1):180–189. <https://doi.org/10.1016/j.ygyno.2018.04.562>
- Cuccia F, D'Alessandro S, Blasi L, Chiantera V, Ferrera G. The role of radiotherapy in the management of vaginal melanoma: a literature review with a focus on the potential synergistic role of immunotherapy. *J Pers Med*. 2023;13(7):1142. <https://doi.org/10.3390/jpm13071142>
- Falcicchio G, Vinci L, Cicinelli E, et al. Vulvar malignant melanoma: a narrative review. *Cancers*. 2022;14(21):5217. <https://doi.org/10.3390/cancers14215217>
- Barcellini A, Vitolo V, Facoetti A, et al. Feasibility of carbon ion radiotherapy in the treatment of gynecological melanoma. *In Vivo*. 2019;33(2):473–476. <https://doi.org/10.21873/invivo.11497>
- Cavaliere S, Ronchi S, Barcellini A, et al. Toxicity of carbon ion radiotherapy and immune checkpoint inhibitors in advanced melanoma. *Radiother Oncol*. 2021;164:1–5. <https://doi.org/10.1016/j.radonc.2021.08.021>
- Murata H, Okonogi N, Wakatsuki M, et al. Tumors TWGOG. Long-term outcomes of carbon-ion radiotherapy for malignant gynecological melanoma. *Cancers*. 2019;11(4):482. <https://doi.org/10.3390/cancers11040482>
- Reid F, Bhatla N, Oza AM, et al. The World Ovarian Cancer Coalition Every Woman Study: identifying challenges and opportunities to improve survival and quality of life. *Int J Gynecol Cancer*. 2021;31(2):238–244. <https://doi.org/10.1136/ijgc-2019-000983>
- Kamada T, Tsujii H, Blakely EA, et al. Carbon ion radiotherapy in Japan: an assessment of 20 years of clinical experience. *Lancet Oncol*. 2015;16(2):e93–e100.

10. Tinganelli W, Durante M. Carbon ion radiobiology. *Cancers*. 2020;12:3022. <https://doi.org/10.3390/cancers12103022>
11. De Ruysscher D, Niedermann G, Burnet NG, Siva S, Lee AWM, Hegi-Johnson F. Radiotherapy toxicity. *Nat Rev Dis Primers*. 2019;5:13.
12. Son B, Kwon T, Lee S, et al. CYP2E1 regulates the development of radiation-induced pulmonary fibrosis via ER stress- and ROS-dependent mechanisms. *Am J Physiol Lung Cell Mol Physiol*. 2017;313:L916–L929.
13. Wang JS, Wang HJ, Qian HL. Biological effects of radiation on cancer cells. *Mil Med Res*. 2018;5(20) <https://doi.org/10.1186/s40779-018-0167-4>
14. Diehn M, Cho RW, Lobo NA, et al. Association of reactive oxygen species levels and radioresistance in cancer stem cells. *Nature*. 2009;458:780–783.
15. Nagelkerke A, Bussink J, van der Kogel AJ, Sweep FC, Span PN. The PERK/ATF4/LAMP3-arm of the unfolded protein response affects radioresistance by interfering with the DNA damage response. *Radiother Oncol*. 2013;108:415–421.
16. Taylor MA, Das BC, Ray SK. Targeting autophagy for combating chemoresistance and radioresistance in glioblastoma. *Apoptosis*. 2018;23:563–575.
17. Lukiewicz S. "Interference with endogenous radioprotectors as a method of radiosensitization in IAEA's modification of radiosensitivity of biological systems." Proceedings of the Advisory Group Meeting on Modification of Radiosensitivity of Biological Systems, International Atomic Energy Agency. 1975.
18. Slominski A, Tobin DJ, Shibahara S, Wortsman J. Melanin pigmentation in mammalian skin and its hormonal regulation. *Physiol Rev*. 2004;84:1155–1228.
19. Brozyna AA, VanMiddlesworth L, Slominski AT. Inhibition of melanogenesis as a radiation sensitizer for melanoma therapy. *Int J Cancer*. 2008;123(6):1448–1456. <https://doi.org/10.1002/ijc.23664>
20. Schwabe K, Lassmann G, Damerau W, Naundorf H. Protection of melanoma cells against msuperoxygen radicals by melanosomes. *J Cancer Res Clin Oncol*. 1989;115:597–600.
21. Ripley S. Is nuclear medicine cost-effective? *Dimens Health Serv*. 1991;68:21–23.
22. Slominski A, Wortsman J, Carlson AJ, Matsuoka LY, Balch CM, Mihm MC. Malignant melanoma. *Arch Pathol Lab Med*. 2001;125:1295–1306.
23. Slominski RM, Zmijewski MA, Slominski AT. The role of melanin pigment in melanoma. *Exp Dermatol*. 2015;24:258–259.
24. Mackintosh JA. The antimicrobial properties of melanocytes, melanosomes and melanin and the evolution of black skin. *J Theor Biol*. 2001;211:101–113.
25. Plonka PM, Passeron T, Brenner M, et al. What are melanocytes really doing all day long. *Exp Dermatol*. 2009;18:799–819.
26. Sarna M, Zadlo A, Hermanowicz P, Madeja Z, Burda K, Sarna T. Cell elasticity is an important indicator of the metastatic phenotype of melanoma cells. *Exp Dermatol*. 2014;23:813–818. <https://doi.org/10.1111/exd.12535>
27. Sarna M, Krzykawska-Serda M, Jakubowska M, Zadlo A, Urbanska K. Melanin presence inhibits melanoma cell spread in mice in a unique mechanical fashion. *Sci Rep*. 2019;9:9280. <https://doi.org/10.1038/s41598-019-45643-9>
28. Krakhamal NV, Zavyalova MV, Denisov EV, Vtorushin SV, Perelmuter VM. Cancer invasion: patterns and mechanisms. *Acta Naturae*. 2015;7(2):17–28.
29. Sniegocka M, Podgórska E, Plonka PM, et al. Transplantable melanomas in hamsters and gerbils as models for human melanoma. Sensitization in melanoma radiotherapy-from animal models to clinical trials. *Int J Mol Sci*. 2018;19:1048. <https://doi.org/10.3390/ijms19041048>
30. Charalampopoulou A, Barcellini A, Frittitta GE, et al. In vitro effects of photon beam and carbon ion radiotherapy on the perineural invasion of two cell lines of neurotropic tumours. *Life*. 2023;13(3):794. <https://doi.org/10.3390/life13030794>. quelli.gia.in.quell.paper.citati
31. Fujita M, Otsuka Y, Yamada S, Iwakawa M, Imai T. X-ray irradiation and Rho-kinase inhibitor additively induce invasiveness of the cells of the pancreatic cancer line MIAPaCa-2, which exhibits mesenchymal amoeboid motility. *Cancer Sci*. 2011;102:792–798.
32. Fujita M, Otsuka Y, Imadome K, Endo S, Yamada S, Imai T. Carbon-ion radiation enhances migration ability and invasiveness of the pancreatic cancer cell PANC-1, in vitro. *Cancer Sci*. 2012;103:677–683.
33. Slominski A. Some properties of Bomirski Ab amelanotic melanoma cells, which underwent spontaneous melanization in primary cell culture. Growth kinetics, cell morphology, melanin content and tumorigenicity. *J Cancer Res Clin Oncol*. 1985;109:29–37. <https://doi.org/10.1007/BF01884251>
34. Kinnaert E, Morandini R, Simon S, Hill HZ, Ghanem G, Van Houtte P. The degree of pigmentation modulates the radiosensitivity of human melanoma cells. *Radiat Res*. 2000;154:497–502. [https://doi.org/10.1667/0033-7587\(2000\)154\[0497:tdopmt\]2.0.co;2](https://doi.org/10.1667/0033-7587(2000)154[0497:tdopmt]2.0.co;2)
35. Rossi S. The National Centre for Oncological Hadrontherapy (CNAO): status and perspectives. *Physica Medica*. 2015;31(4):333–351. <https://doi.org/10.1016/j.ejmp.2015.03.001>
36. Baselet B, Sonveaux P, Baatout S, Aerts A. Pathological effects of ionizing radiation: endothelial activation and dysfunction. *Cell Mol Life Sci*. 2019;76(4):699–728. <https://doi.org/10.1007/s00018-018-2956-z>
37. Limame R, Wouters A, Pauwels B, et al. Comparative analysis of dynamic cell viability, migration and invasion assessments by novel real-time technology and classic endpoint assays. *PLoS One*. 2012;7(10):e46536. <https://doi.org/10.1371/journal.pone.0046536>
38. Kollias N, Sayre RM, Zeise L, Chedekel MR. Photoprotection by melanin. *J Photochem Photobiol B*. 1991;9:135–160.
39. Meyskens Jr FL, Farmer P, Fruehauf JP. Redox regulation in human melanocytes and melanoma. *Pigment Cell Res*. 2001;14:148–154.
40. Pawelek JM, Chakraborty AK, Osber MP, et al. Molecular cascades in UV-induced melanogenesis: a central role for melanotropins? *Pigment Cell Res*. 1992;5:348–356.
41. Smit NP, Vink AA, Kolb RM, et al. Melanin offers protection against induction of cyclobutane pyrimidine dimers and 6-4 photoproducts by UVB in cultured human melanocytes. *Photochem Photobiol*. 2001;74:424–430.
42. Wood JM, Jimbow K, Boissy RE, et al. What's the use of generating melanin? *Exp Dermatol*. 1999;8:153–164.
43. Brenner M, Hearing VJ. The protective role of melanin against UV damage in human skin. *Photochem Photobiol*. 2008;84(3):539–549. <https://doi.org/10.1111/j.1751-1097.2007.00226.x>
44. D'Orazio J, Jarrett S, Amaro-Ortiz A, Scott T. UV radiation and the skin. *Int J Mol Sci*. 2013;14(6):12222–12248. <https://doi.org/10.3390/ijms140612222>
45. Quaresma JAS. Organization of the skin immune system and compartmentalized immune responses in infectious diseases. *Clin Microbiol Rev*. 2019;32(4):e00034-18. <https://doi.org/10.1128/CMR.00034-18>
46. Ballester Sánchez R, de Unamuno Bustos B, Navarro Mira M, Botella Estrada R. Actualización en melanoma mucoso. *Actas Dermosifiliogr*. 2015;106:96–103. <https://doi.org/10.1016/j.adengl.2014.12.008>
47. Upadhyay PR, Starner RJ, Swope VB, Wakamatsu K, Ito S, Abdel-Malek ZA. Differential induction of reactive oxygen species and expression of antioxidant enzymes in human melanocytes correlate with melanin content: implications on the response to solar UV and melanoma susceptibility. *Antioxidants*. 2022;11(6):1204. <https://doi.org/10.3390/antiox11061204>
48. Emanuelli M, Sartini D, Molinelli E, et al. The double-edged sword of oxidative stress in skin damage and melanoma: from physiopathology to therapeutical approaches. *Antioxidants*. 2022;11(4):612. <https://doi.org/10.3390/antiox11040612>
49. Bento-Lopes L, Cabaço LC, Charneca J, Neto MV, Seabra MC, Barral DC. Melanin's journey from melanocytes to keratinocytes: uncovering the molecular mechanisms of melanin transfer and processing. *Int J Mol Sci*. 2023;24(14):11289. <https://doi.org/10.3390/ijms241411289>
50. Hara M, Yaer M, Gilchrist BA. Endothelin-1 of keratinocyte origin is a mediator of melanocyte dendricity. *J Invest Dermatol*. 1995;105:744–748. <https://doi.org/10.1111/1523-1747.ep12325522>
51. Banerjee SS, Harris M. Morphological and immunophenotypic variations in malignant melanoma. *Histopathology*. 2000;36:387–402. <https://doi.org/10.1046/j.1365-2559.2000.00894.x>
52. Kamiński K, Kazimierzczak U, Kolenda T. Oxidative stress in melanogenesis and melanoma development. *Contemp Oncol*. 2022;26(1):1–7. <https://doi.org/10.5114/wo.2021.112447>
53. Slominski A, Paus R, Mihm MC. Inhibition of melanogenesis as an adjuvant strategy in the treatment of melanotic melanomas: selective review and hypothesis. *Anticancer Res*. 1998;18:3709–3715.
54. Ananditha KP, Weber KJ, Brons S, Debus J, Hauswald H. In vitro sensitivity of malignant melanoma cells lines to photon and heavy ion radiation. *Clin Transl Radiat Oncol*. 2019;17:51–56. <https://doi.org/10.1016/j.ctro.2019.06.002>
55. Turick CE, Ekechukwu AA, Milliken CE, Casadevall A, Dadachova E. Gamma radiation interacts with melanin to alter its oxidation-reduction potential and results in electric current production. *Bioelectrochemistry*. 2011;82:69–73. <https://doi.org/10.1016/j.bioelechem.2011.04.009>
56. Tugay TI, Zheltonozhskaya MV, Sadovnikov LV, Tugay AV, Farfán EB. Effects of ionizing radiation on the antioxidant system of microscopic fungi with radioadaptive properties found in the Chernobyl exclusion zone. *Health Phys*. 2011;101:375–382. <https://doi.org/10.1097/HP.0b013e3181f56bf8>
57. Burraco P, Orizaola G. Ionizing radiation and melanism in Chornobyl tree frogs. *Evol Appl*. 2022;15(9):1469–1479. <https://doi.org/10.1111/eva.13476>
58. Dadachova E, Casadevall A. Ionizing radiation: how fungi cope, adapt, and exploit with the help of melanin. *Curr Opin Microbiol*. 2008;11:525–531. <https://doi.org/10.1016/j.mib.2008.09.013>
59. Cabaço LC, Tomás A, Pojo M, Barral DC. The dark side of melanin secretion in cutaneous melanoma aggressiveness. *Front Oncol*. 2022;12:887366. <https://doi.org/10.3389/fonc.2022.887366>
60. Kohli K, Pillarisetty VG, Kim TS. Key chemokines direct migration of immune cells in solid tumors. *Cancer Gene Ther*. 2022;29(1):10–21. <https://doi.org/10.1038/s41417-021-00303-x>
61. Helm A, Fournier C. High-LET charged particles: radiobiology and application for new approaches in radiotherapy. *Strahlenther Onkol*. 2023;199(12):1225–1241. <https://doi.org/10.1007/s00066-023-02158-7>
62. Ronchi S, Cicchetti A, Bonora M, et al. Curative carbon ion radiotherapy in a head and neck mucosal melanoma series: facing the future within multidisciplinary. *Radiother Oncol*. 2023;190:110003. <https://doi.org/10.1016/j.radonc.2023.110003>
63. Saud A, Sagineedu SR, Ng H, Stanslas J, Lim JC. Melanoma metastasis: what role does melanin play? (Review). *Oncol Rep*. 2022;48:217.